

# Poor man's topological quantum memory based on the Su-Schrieffer-Heeger chain

(Dated: February 28, 2018)

Topological properties of quantum systems could provide efficient protection against environmental noise, and thereby drastically advance the potential of these setups for applications in quantum information processing. Most proposals in topological quantum information are based on many-body systems, e.g., fractional quantum Hall systems, exotic superconductors, or ensembles of interacting spins, bearing an inherent conceptual complexity. In this lecture, we propose and study a simpler model for a topological quantum memory, based on the single-particle tight-binding Hamiltonian known as the Su-Schrieffer-Heeger model. In this model, the qubit is protected only against perturbations that have chiral symmetry. Apart from that, this model shows the principal feature expected from a topological quantum memory: although it is assembled from noisy building blocks, its performance improves (i) if the number of its building blocks is increased, or (ii) if the protecting energy gap is increased. Furthermore, we present small-scale numerical simulations to demonstrate the following features: (iii) The performance of the memory is ultimately limited by the noise acting during the information transfer to and from the memory. (iv) To minimize the impact of noise during information transfer, one might have to optimize between slow transfer, which gives noise ample time to erase information, and fast transfer, which induces leakage from the topological memory subspace. We expect these features to be generic, and to inevitably arise in more complex models and experimental realizations of topological quantum memories.

## CONTENTS

Contributors	1
I. Hopping noise erases the information in a charge qubit	1
II. Noiseless charge qubit can be used as a quantum memory	3
III. A slightly noisy quantum memory	5
IV. Zero-energy edge states of the SSH model are robust against hopping disorder	5
V. SSH chain as a quantum memory	7

## CONTRIBUTORS

Writeup: Andras Palyi. Numerics, figures, discussions: Laszlo Oroszlany, Peter Boross, Janos Asboth.

### I. HOPPING NOISE ERASES THE INFORMATION IN A CHARGE QUBIT

1. *Charge qubit.* Two sites, e.g., a double quantum dot. Single-electron basis states  $|L\rangle$ ,  $|R\rangle$ . The two sites are occupied by a single electron. Model Hamiltonian:

$$H = \frac{\epsilon}{2}\sigma_z + v\sigma_x, \quad (1)$$

where the Pauli matrices are defined as, e.g.,  $\sigma_z = |L\rangle\langle L| - |R\rangle\langle R|$ . On-site energy difference  $\epsilon$ , hopping amplitude  $v$ .

2. *Charge Rabi oscillations.* A simple example of the dynamics of the charge qubit is as follows. Consider  $\epsilon = 0$  and  $v > 0$ , e.g.,  $v = 10 \mu\text{eV}$ , which is a reasonable value for a realistic double quantum dot. Prepare the initial state as  $|\psi_0\rangle = |L\rangle$ . Describe the dynamics, e.g., calculate the time evolution of the occupation probability of the right site, that is,  $P_R(t) \equiv |\langle R|\psi(t)\rangle|^2 = ?$  Straightforward calculation shows that  $|\psi(t)\rangle = \cos(vt/\hbar)|L\rangle - i\sin(vt/\hbar)|R\rangle$ , and thereby  $P_R(t) = \sin^2(vt/\hbar)$ . That is, the electron oscillates coherently between the two sites. We call this simple dynamics *charge Rabi oscillations*. A complete cycle of those oscillations takes  $t_{\text{Rabi}} = h/2v$  time. For  $v = 10 \mu\text{eV}$ , we have  $t_{\text{Rabi}} \approx 0.2 \text{ ns}$ .

3. *Noise makes the charge-qubit state mixed.* Noise, e.g., electric-field fluctuations, induce an uncontrolled, random contribution to the charge-qubit Hamiltonian, leading to uncontrolled dynamics of the qubit state and hence to loss of information. One simple way to describe such processes is to account for the noise via the Hamiltonian

$$H_{\text{noise}}^{(j)} = \xi_x^{(j)}(t)\sigma_x + \xi_y^{(j)}(t)\sigma_y + \xi_z^{(j)}(t)\sigma_z, \quad (2)$$

where the functions  $\xi_\alpha^{(j)}(t)$  are random functions of time, characterized by a ‘parameter’ or ‘index’ of realizations  $j$ . Different noise realizations can have different probabilities, encoded in the probability density function (pdf)  $P(j)$ , which has to fulfill  $\sum_j P(j) = 1$  (if  $j$  is a discrete index) or  $\int dj P(j) = 1$  (if  $j$  is a continuous parameter). The evolution of the initial state  $|\psi_0\rangle$  depends on the noise realization. To get a statistical description of the time evolution, one can use the density matrix:

$$\rho(t) = \sum_j P(j) |\psi^{(j)}(t)\rangle \langle \psi^{(j)}(t)|, \quad (3)$$

where  $\psi^{(j)}(t)$  is the pure time-evolving state subject to noise realization  $j$ . Of course this  $\rho(t)$  describes a mixed state in general. (Note that this noise model is ‘classical’ in the sense that entanglement with the quantum degrees of freedom of the environment is not taken into account.)

4. *Fidelity.* To describe the state-preserving quality of a charge qubit subject to noise, we use the concept of fidelity. Fidelity between a pure quantum state  $|\psi_0\rangle$  and a mixed quantum state  $\rho(t)$  can be defined as

$$F(t) = \sqrt{\langle \psi_0 | \rho(t) | \psi_0 \rangle}. \quad (4)$$

An example: if  $\rho(t)$  is the same state as  $|\psi_0\rangle$ , that is, if  $\rho(t) = |\psi_0\rangle \langle \psi_0|$ , then  $F = 1$ . If they are unequal, then their fidelity is less than 1. In particular, if  $\rho(t)$  is completely mixed, i.e.,  $\rho(t) = \frac{1}{2} |\psi_0\rangle \langle \psi_0| + \frac{1}{2} |\psi_0^\perp\rangle \langle \psi_0^\perp|$  with  $\langle \psi_0 | \psi_0^\perp \rangle = 0$ , then  $F(t) = 1/\sqrt{2} \approx 0.707$ . Note that this example reveals that a  $\sim 70\%$  fidelity means that the information encoded in the qubit is completely lost.

5. *Hopping noise leads to complete information loss.* To provide a concrete example of the concepts introduced above, we consider a very simple noise model for our charge qubit. We call that *Gaussian quasistatic hopping noise*. We assume that we intentionally tune our Hamiltonian parameters to zero, but there is an uncontrolled source of noise which induces a random contribution to the hopping amplitude. Hence, our noise Hamiltonian reads

$$H_{\text{noise}}^{(v)} = v\sigma_x. \quad (5)$$

Here, our noise parameter (denoted as  $j$  above in the general discussion) is  $v$ . We assume that  $v$  is time-independent during a single run of the time evolution, but can change randomly between two subsequent runs (hence the name *quasistatic*), and its randomness is characterized by a Gaussian pdf,

$$P(v) = G(0, \sigma, v), \quad (6)$$

where we use the notation  $G(\mu, \sigma, x)$  for the Gaussian pdf for variable  $x$  with mean  $\mu$  and standard deviation  $\sigma$ :

$$G(\mu, \sigma, x) = \frac{1}{\sqrt{2\pi}\sigma} e^{-\frac{(x-\mu)^2}{2\sigma^2}}. \quad (7)$$

The task now is to characterize information loss due to this noise. Take the left-localized initial state for concreteness,  $|\psi_0\rangle = |L\rangle$ . We have already solved the time evolution for a fixed hopping amplitude. Utilizing that, and following the generic statistical averaging procedure described above, we find

$$F(t) = \sqrt{\frac{1 + e^{-2t^2\sigma^2/\hbar^2}}{2}}. \quad (8)$$

For  $t = 0$ , we have  $F(t) = 1$ , as expected. For long times  $t \rightarrow \infty$ , we have  $F(t) = 1/\sqrt{2}$ , i.e., information encoded in the charge qubit is completely lost. The crossover between the two values, i.e., the loss of information, happens

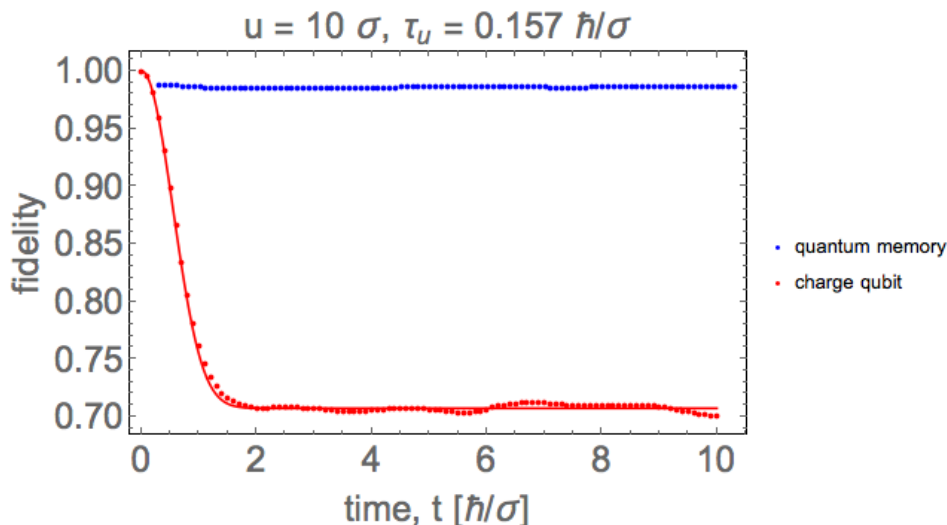


FIG. 1. Information is lost if encoded in a noisy charge qubit (red), but can be preserved if transferred to a noiseless memory (blue).

on the time scale  $t_{\text{loi}} = \hbar/\sigma$ . Note that we could have reached this conclusion just using dimensional analysis: the only energy scale in our problem is  $\sigma$ , therefore the only characteristic time scale is  $\hbar/\sigma$ . This is sometimes called *qubit lifetime*. (In certain noise models similar to this one, this time scale is sometimes called *inhomogeneous dephasing time*, and is denoted by  $T_2^*$ .) The numerical value of this time scale, for hopping noise strength  $\sigma = 1 \mu\text{eV}$ , is  $t_{\text{loi}} \approx 0.658 \text{ ns}$ . The analytical result (8) is shown as the red solid line in Fig. 1. The red dots show the result of a Monte Carlo check, when we draw 5000 random values of  $v$  using a Gaussian pdf, determine the time evolution for each realization, construct the density matrix from those, and evaluate the fidelity from that density matrix. The solid red line and the red dots show a reasonable agreement.

6. *Exercise.* Work out the fidelity evolution  $F(t)$  for the initial states  $|\psi\rangle = (|L\rangle + |R\rangle)/\sqrt{2}$  and  $|\psi\rangle = (|L\rangle + i|R\rangle)/\sqrt{2}$ .

## II. NOISELESS CHARGE QUBIT CAN BE USED AS A QUANTUM MEMORY

1. *An elementary quantum memory.* We have just seen that we can prepare an arbitrary quantum state in our noisy charge qubit, but the information gets lost due to the uncontrolled tunneling noise. Assume that we have a noiseless charge qubit, which we can use to hide the information in the noisy charge qubit, and thereby prolong the lifetime of the prepared quantum state. A simple scheme for this is shown in Fig. 2. There, the red dots represent the noisy charge qubit, and the blue ones represent a noiseless one which is used as a quantum memory. We will use  $|L'\rangle$  and  $|R'\rangle$  to denote the single-electron states localized on the left and right sites of the memory. It is assumed that we prepare an arbitrary quantum state  $|\psi_0\rangle$  in the noisy qubit, at  $t = 0$ , as shown in the figure. By switching on tunneling  $u$  between  $|L\rangle$  and  $|L'\rangle$ , and similarly between  $|R\rangle$  and  $|R'\rangle$  for an appropriately chosen time interval  $\tau_u$ , we expect to transfer the qubit state from the noisy one to the memory ('store'), simply via a half charge Rabi oscillation. Once the qubit state is transferred and hidden from noise in the memory, we can wait for some time  $\tau_{\text{wait}}$ , transfer the information back to the qubit ('retrieve') with the same transfer pulse, and hope that the state has been preserved.
2. *Timing of the transfer pulse.* The transfer pulse  $u(t)$  applied for storage and retrieval should force the electron to make a half charge Rabi oscillation, say, between  $|L\rangle$  and  $|L'\rangle$ . The complete Hamiltonian in the  $|L\rangle, |R\rangle, |L'\rangle, |R'\rangle$  basis reads

$$H(t) = \begin{pmatrix} 0 & v & u(t) & 0 \\ v & 0 & 0 & u(t) \\ u(t) & 0 & 0 & 0 \\ 0 & u(t) & 0 & 0 \end{pmatrix}. \quad (9)$$

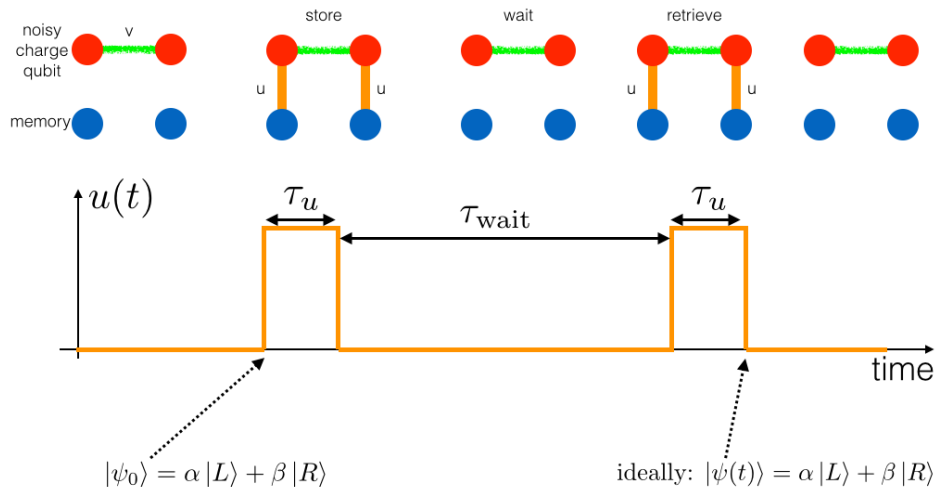


FIG. 2. A noiseless memory, and a simple protocol for storage and retrieval.

The time dependence of the transfer hopping amplitude  $u(t)$  is shown in the bottom panel of Fig. 2. As before,  $v$  is a random hopping amplitude attributed to Gaussian quasistatic hopping noise. According to the above discussion on charge Rabi oscillations, the transfer time  $t_u$  and transfer pulse strength  $u$  should satisfy  $u\tau_u/\hbar = \pi/2$ , implying the relation

$$\tau_u = \frac{\hbar}{4u}. \quad (10)$$

For a transfer pulse strength  $u = 10 \mu\text{eV}$ , we find  $\tau_u \approx 0.1$  ns. If the hopping noise has the strength  $\sigma = 1 \mu\text{eV}$  as above, then we expect that this choice of  $u$  will be sufficient to store in the memory before the qubit gets lost in the noisy qubit, since  $\tau_u \approx 0.1 \text{ ns} < t_{\text{loi}} \approx 0.658 \text{ ns}$ . Increasing the transfer pulse strength  $u$  further is expected to yield a faster transfer and thereby a better memory functionality of this setup.

3. *This quantum memory works.* The time dependence of the qubit fidelity  $F(t)$ , for the case when we use the noiseless charge qubit as a memory, is shown as the blue data set in Fig. 1. Here we use the Monte Carlo simulation described above, with 5000 realizations. Note that the leftmost point of this data set belongs to time  $t = 2\tau_u \approx 0.314 \hbar/\sigma$ , the sum of the times required for storage and retrieval, since that is the minimum time window between the preparation and the measurement when we are using the memory. The data set shows that the memory works: instead of complete information loss within the time frame  $\hbar/\sigma$ , information is conserved to a large extent, signalled by a ‘fidelity plateau’ at around 0.98. The plateau height does not decrease with time, (although small-amplitude oscillations can be seen due to the finite size of the random sample): once we transfer the qubit state to the noiseless memory, we switch off information loss, so we can wait for an arbitrarily long  $\tau_{\text{wait}}$  without any further loss of information.
4. *Fidelity plateau height is the figure of merit for the memory.* From the above discussion, it seems that the quality of the memory can be characterized by a single figure of merit, the height of the fidelity plateau, taking the value  $\approx 98\%$  in Fig. 1. In Fig. 3, we compare the fidelity time evolution for three different values of the transfer pulse strength. The results indicate that, indeed, by increasing the transfer pulse strength  $u$  and thereby shortening the transfer time  $\tau_u = \hbar/(4u)$ , we obtain a higher fidelity plateau, hence a better memory.
5. *The limit of a perfect memory.* How to set the transfer pulse strength  $u$  to optimize the memory, that is, to maximize the height of the fidelity plateau? The choice  $u \rightarrow \infty$  seems to be optimal, since this choice means

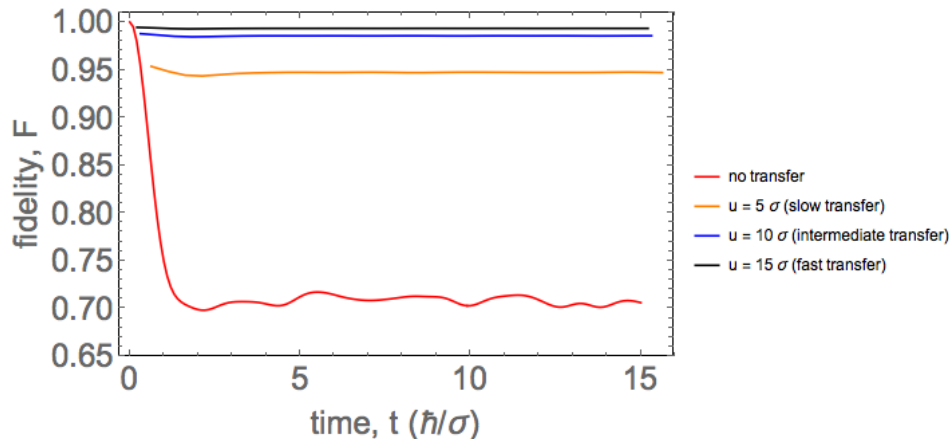


FIG. 3. The figure of merit for the memory is the height of the fidelity plateau; a faster transfer pulse results in a better memory.

infinitely fast storage and retrieval, implying that the noise has no time to induce any uncontrolled dynamics. That also means that the choice  $u \rightarrow \infty$  in our model leads to a *perfect* memory: the fidelity plateau height converges to 1 in that case.

6. *Exercise.* Determine the fidelity decay in the model described above for the initial state  $|\psi_0\rangle = \sqrt{\frac{2}{3}}|L\rangle + \sqrt{\frac{1}{3}}|R\rangle$ , for the case when the memory is not used, and for the case when the memory is used with a transfer pulse strength  $u = 10\sigma$ .
7. *A remark on spin echo.* In reality, the information loss due to quasistatic noise is not as harmful as described above: often this effect can be eliminated to some extent using control techniques related to or derived from the ‘spin echo’ trick applied in paramagnetic resonance.

### III. A SLIGHTLY NOISY QUANTUM MEMORY

1. *Fidelity plateau duration as a second figure of merit of the memory.* Our previous model was based on a completely noiseless memory, leading to a fidelity plateau that does not decay with time. Some noise in the memory changes that behavior, and defines a time scale after which the fidelity plateau breaks down. This is illustrated by a simple extension of our model, where the memory is also subject to hopping noise, similar to that on the noisy charge qubit, but with a smaller strength  $\sigma'$ . The fidelity time evolution  $F(t)$  for  $u = 10\sigma$ , and a few representative values of the memory noise strength  $\sigma'$ , is shown in Fig. 4. In each case, the fidelity plateau height is the same, around 98%, but the duration gets shorter as the noise strength increases.

### IV. ZERO-ENERGY EDGE STATES OF THE SSH MODEL ARE ROBUST AGAINST HOPPING DISORDER

1. *Edge state in a topological half-infinite SSH chain.* Chapter 1 of the lecture notes of the first semester, see <https://arxiv.org/abs/1509.02295>, provides an introduction to the Su-Schrieffer-Heeger (SSH) model. We will denote the intracell hopping with  $v$ , and the intercell hopping with  $w$ . Recall that the case  $v > w$  is called the trivial phase, whereas the  $v < w$  case is called the topological phase. A half-infinite topological SSH chain with a single open end hosts a zero-energy bound state localized to its end. The bound state is sublattice-polarized, and has an exponentially decaying spatial dependence toward the bulk, with penetration depth  $\xi = -1/\log(v/w)$ .
2. *Left and right edge states hybridize in a finite open SSH chain.* Consider a finite topological SSH chain with open ends. Denote the number of unit cells as  $N_c$ . In the fully dimerized limit  $v = 0$ , there are two edge states at the two ends, each of them perfectly localized to a single site, exactly at zero energy. For finite  $v$ , these two states acquire a finite penetration depth  $\xi$  (see above), and thereby hybridize, forming a bonding and an

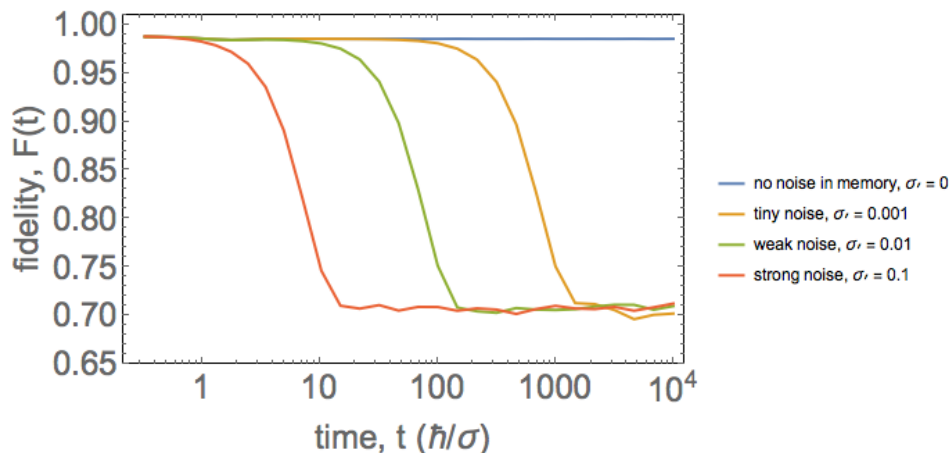


FIG. 4. Fidelity plateau duration as a second figure of merit for the memory: a more noisy memory has a shorter plateau.

antibonding energy eigenstate, whose distance in energy (the ‘minigap’  $\Delta$ ) is small as long as the chain is long or the intercell hopping  $v$  is small. In fact, the minigap scales as  $\Delta \propto e^{-N_c/\xi}$ , hence the minigap decreases as the chain length  $N_c$  grows or if the hopping ratio  $v/w$  decreases.

3. *The edge states and their zero-energy nature is protected by size and symmetry.* In Chapter 1.5 of the lecture notes of the first semester, we describe the smallness of the minigap and the robustness of the edge states in the presence of hopping disorder, which preserves chiral symmetry. Here we reinforce this finding. As long as chiral symmetry is present, the energy of a single edge state cannot be replaced by disorder from zero as long as this edge state does not hybridize with the other edge state. This is because chiral symmetry guarantees the up-down symmetry of the energy spectrum, hence the eigenvalue of a spatially isolated zero-energy eigenstate must stick to zero, no matter how the Hamiltonian is deformed, as long as Hamiltonian has chiral symmetry. This implies that the two zero eigenvalues can leave zero only due to the hybridization of the two edge states, which is weak due to their exponential localization. Therefore, the minigap opened by the hybridization is also small. Note, however, that as soon as disorder breaks chiral symmetry (e.g., the on-site energies are disordered), then the up-down symmetry of the spectrum is no longer guaranteed, and therefore even a spatially isolated edge state can acquire a nonzero energy. The simplest example is the energy eigenvalue of a perfectly localized edge state in the topological fully dimerized limit, which is given by the random on-site potential at the site where the state is localized.
4. *Numerical demonstration of the robust two-dimensional zero-energy subspace.* The left panel of Fig. 5 shows the energy spectrum for many different random realizations of SSH chains with hopping disorder. The length of the chain is  $N_c = 10$  unit cells. The Hamiltonians are drawn from a random ensemble, where the on-site energies are zero, the intracell hoppings  $v_m$  ( $m = 1, \dots, N_c$ ) are independent Gaussian variables centered around zero, with pdf  $G(0, \sigma, v_m)$ , and the intercell hoppings  $w_m$  ( $m = 1, \dots, N_c - 1$ ) are independent Gaussian variables, centered around  $w$ , with pdf  $G(w, \sigma, w_m)$ . That is, the strength of the disorder is characterized by the ratio  $\sigma/w$ . In the plot, for each disorder strength  $\sigma$ , we draw a random  $20 \times 20$  Hamiltonian according to the above rule, and plot its 20 eigenvalues. Furthermore, we use a red color to indicate eigenvalues corresponding to edge states: the point is red if the corresponding eigenstate is at least 75% localized in the two edge unit cells, and black otherwise. From the plot it is apparent that even for disorder strength of  $\sigma \approx 0.3w$ , the zero-energy states are well localized, stay around zero energy, and are energetically well separated from the other, delocalized states. The right panel illustrates that disorder not preserving chiral symmetry is efficient in pushing the edge states away from zero energy. Here, the hoppings are ordered, but the on-site energies  $\epsilon_{A,B}$  are independent Gaussian random variables with pdf  $G(0, \Sigma, \epsilon_{A,B})$ . The conclusion here is that as long as only chiral-symmetry-preserving disorder is present, then the two-dimensional zero-energy subspace spanned by the edge-localized states is hardly sensitive to disorder, and thereby we might expect to utilize this subspace as a good quantum memory.

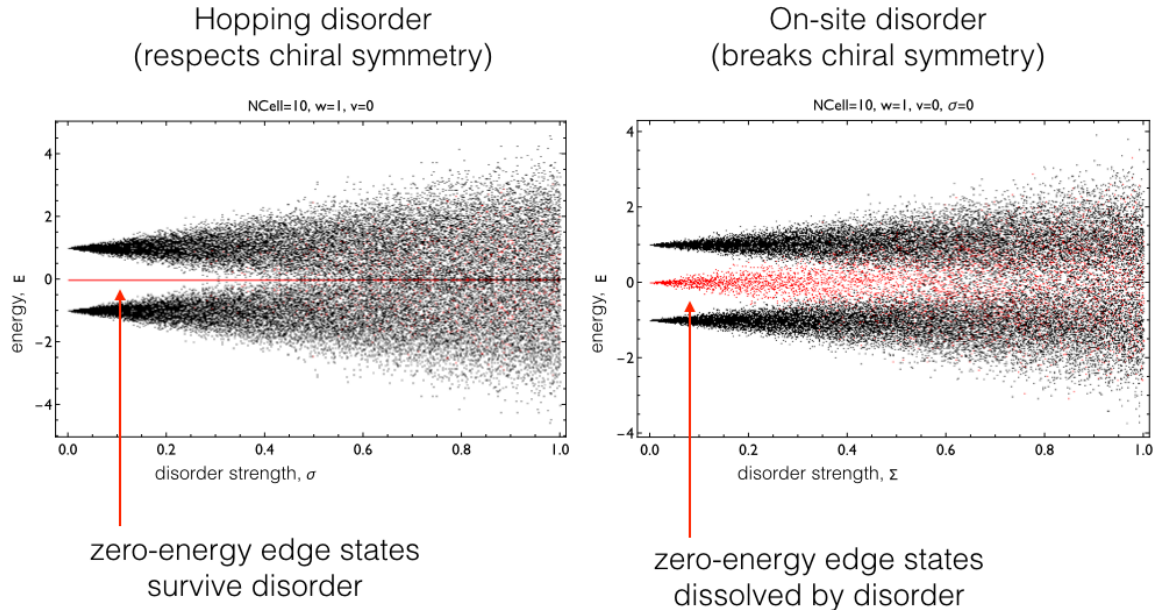


FIG. 5. **Zero-energy edge states survive hopping disorder, which respects chiral symmetry, but are dissolved by on-site disorder, which breaks chiral symmetry.** [Data and figure: Peter Boross]

## V. SSH CHAIN AS A QUANTUM MEMORY

1. *Qubit transfer between the charge qubit and the zero-energy subspace of the SSH chain.* We have seen that a noisy charge qubit has a finite lifetime. Here, we demonstrate that if we assemble a number of such noisy charge qubits to a finite SSH chain, then the latter will function as a much less noisy quantum memory, offering a significantly increased lifetime compared to the single charge qubit. We propose to use an open SSH chain as a memory, using the following scheme. The left (right) site of the noisy charge qubit should be tunnel-coupled to the left (right) end of the SSH chain. In the simplest example of a two-unit-cell chain,  $N_c = 2$ , the Hamiltonian of the qubit + memory setup reads

$$H = \begin{pmatrix} 0 & v & u(t) & 0 & 0 & 0 \\ v & 0 & 0 & 0 & 0 & u(t) \\ u(t) & 0 & 0 & v_1 & 0 & 0 \\ 0 & 0 & v_1 & 0 & w_1 & 0 \\ 0 & 0 & 0 & w_1 & 0 & v_2 \\ 0 & u(t) & 0 & 0 & v_2 & 0 \end{pmatrix} \quad (11)$$

where the basis states are  $|L\rangle, |R\rangle, |1, A\rangle, |1, B\rangle, |2, A\rangle, |2, B\rangle$ . The protocol for the thought experiment is the same as described above:  $u(t)$  is switched on as a square pulse both for storage and retrieval. We assume that the noise strength is the same on the charge qubit and the SSH chain, and consider the case when the SSH chain would be tuned to the fully dimerized limit in the absence of noise. That means, quasistatic Gaussian hopping noise is characterized by a single noise strength  $\sigma$ , via the pdfs  $G(0, \sigma, v)$ ,  $G(0, \sigma, v_m)$  and  $G(w, \sigma, w_m)$ .

2. *The SSH memory does work.* This is illustrated in Fig. 6, where the Monte Carlo time evolution of the fidelity is shown for increasing chain length  $N_c$  (from left to right) and increasing transfer pulse strength  $u$  (from bottom to top). The data clearly demonstrates that the memory works, and gets better as the chain length increases or as the transfer pulse strength increases. In the former case, the fidelity plateau duration increases; in the latter case, the fidelity plateau height increases. It is expected (but we do not show here) that by increasing the noise strength  $\sigma$ , we would see a decrease in both the height and the duration of the fidelity plateau.
3. *Cannot approach perfection with this noisy SSH memory.* A perfect memory is characterized by a fidelity plateau that has unit height and infinite duration. We have seen above that a noiseless charge qubit is a perfect quantum memory in the limit of an infinitely long transfer pulse. Can our protocol based on the SSH chain

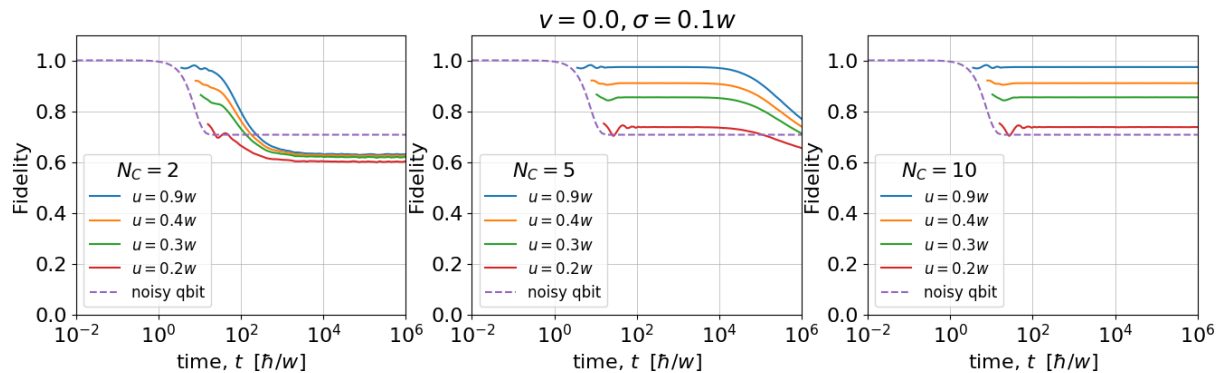


FIG. 6. **Topological quantum memory based on the SSH chain: prolonging the chain increases the fidelity plateau length (from left to right), faster transfer increases the fidelity plateau height (from bottom to top).** [Data and figure: Laszlo Oroszlany]

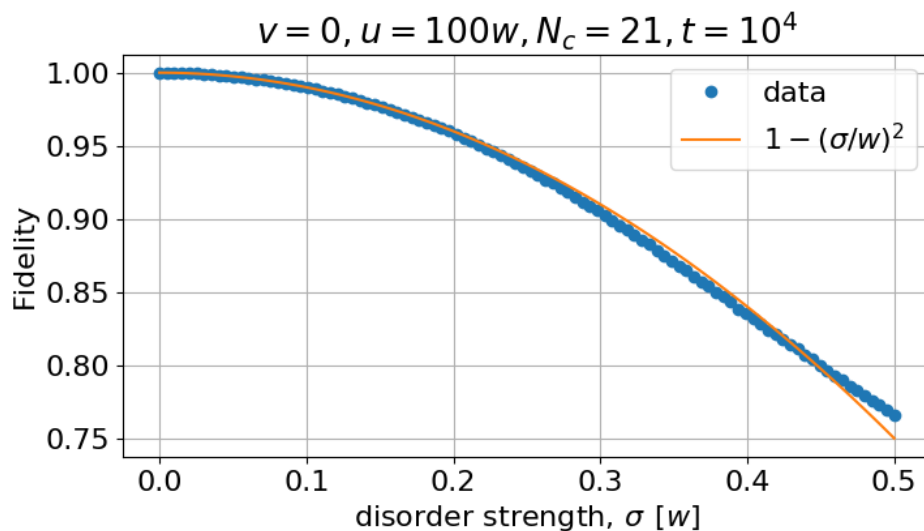


FIG. 7. **Disorder strength sets an upper limit of the achievable fidelity in an SSH quantum memory.** [Data and figure: Laszlo Oroszlany]

lead to a perfect memory? The answer is no. (i) For a fixed  $\sigma$ , the fidelity plateau duration approaches infinity for  $v = 0$ ,  $N_c \rightarrow \infty$ , and  $u \rightarrow \infty$ , which points toward perfection; (ii) but the fidelity plateau height remains below 1. Claim (i) is based on the exponential suppression of the minigap with system size: that implies that as  $N_c \rightarrow \infty$ , the minigap approaches zero, and thereby disorder does not induce any uncontrolled dynamics during the waiting time  $\tau_{\text{wait}}$ . Claim (ii) is illustrated by Fig. 7, where the height of the fidelity plateau is plotted as a function of disorder strength. As seen in the figure, for weak disorder  $\sigma \ll w$ , and fast transfer  $u \gg w$ , the fidelity plateau height is approximately  $1 - (\sigma/w)^2$ , i.e., it remains below unity for finite disorder strength  $\sigma$ . This analytical result can be derived using a combination of two considerations; we leave this derivation as an exercise: (1) the edge state is slightly delocalized to the finite hopping noise, and this delocalization can be described by first-order textbook perturbation theory; (2) when a fast transfer pulse ( $u \gg w, \sigma$ ) is applied, e.g., for the initial state  $|L\rangle$ , then the state after the pulse is not the left edge state of the SSH chain, but the  $|1, A\rangle$  state.

#### 4. Discussion.

(1) Fig. 6 illustrates that for  $v = 0$ , the memory gets better as the transfer pulse strength  $u$  is increased. In other words, the fidelity plateau height increases monotonically with increasing  $u$ . One may wonder: is that true also when  $v$  is nonzero? One might expect that a too strong transfer pulse might induce transitions outside the two-dimensional zero-energy subspace, thereby reducing the fidelity.



(2) Item (1) triggers the question: isn't it possible to improve the quality of storage and retrieval by a pulse shape  $u(t)$  which is better than the square pulse used here? Perhaps designing some less trivial spatial dependence of the tunnel coupling between the qubit and the memory can also be helpful.

(3) Why call the SSH memory 'topological'? 'Topological quantum memory' is often used in the context of error-correction codes. There, the adjective 'topological' often refers to the property of the size-parametrized family that the robustness (fault tolerance) of the code grows with the size of the code. This size-dependence also holds for the SSH memory. In the topological codes, the fault tolerance is usually not related to any symmetries though; this is therefore one point where the analogy between the SSH quantum memory and the topological codes break down: in SSH, the chiral symmetry of the disorder is required for the robustness of the memory.

(4) Of course, it is difficult to envision a physical system where hopping disorder is significant but on-site disorder is suppressed. Therefore, we do not claim that the SSH memory is a practical solution to the real-world problem of making a quantum memory. However, it serves as an extremely simple toy model to illustrate concepts of topological quantum bits, most importantly the size- and symmetry-protected nature. Those are key concepts in more advanced and hopeful schemes, such as topological qubits based on topological superconductors ('Majorana qubits').

(5) Clearly, quasistatic noise treated here is just one particularly simple noise model. In realistic situations, noise is explicitly time dependent, or even has quantum features; an important extension of the present discussion is to consider those noise characteristics.